Conf-931108--45

Note: This is a preprint of a paper being submitted for publication. Contents of this paper should not be quoted nor referred to without permission of the author(s).

Paper to be presented to 93 Fall MRS Meeting

COLLOIDAL Au NANOCLUSTERS FORMED IN FUSED SILICA BY MeV ION IMPLANTATION AND ANNEALING

C. W. White, D. S. Zhou, J. D. Budai, and R. A. Zuhr
Oak Ridge National Laboratory
Oak Ridge, Tenn.

R. H. Magruder and D. H. Osborne
Vanderbilt University
Nashville, Tenn.

NOTE: This manuscript will be put in camera-ready format following review.

Prepared by the
Oak Ridge National Laboratory
Oak Ridge, Tennessee 37831
managed by
MARTIN MARIETTA ENERGY SYSTEMS, INC.
for the
U.S. DEPARTMENT OF ENERGY
under contract DE-AC05-84OR21400

November 1993

MASTER

COLLOIDAL Au NANOCLUSTERS FORMED IN FUSED SILICA BY MeV ION IMPLANTATION AND ANNEALING

C. W. WHITE,* D. S. ZHOU,* J. D. BUDAI,* R. A. ZUHR,* R. H. MAGRUDER,** AND D. H. OSBORNE**
*Oak Ridge National Laboratory, P. O. Box 2008, Oak Ridge, Tennessee 37831-6057
**Vanderbilt University, Nashville, Tennessee

ABSTRACT

MeV implantation of Au has been used to create a high density of Au nanoclusters in the near surface of fused silica. Measurements of the nanocluster size and size distribution under various implantation/annealing conditions are presented and correlated with measurements of optical absorption arising from surface plasmon resonance absorption by the Au nanoclusters in fused silica. Preliminary measurements of the nonlinear refractive index are included.

INTRODUCTION

Glasses containing Au colloidal nanoclusters have attracted interest recently due to their nonlinear optical properties.[1,2] The third-order optical susceptibility is large, and the nonlinear optical response time is in the picosecond regime. Ion implantation has been shown to produce a high density of Au colloids in glasses[3-6] and other materials.[7,8] Colloid volume fraction of several percent have been reported, which is much higher than that which can be obtained in Au doped glass (~0.1%). The high-precipitate volume fraction and small nanocluster size leads to values for the third-order susceptibility that are much greater than those for Au doped glass.[4,5,9] This has stimulated recent interest in the use of ion implantation to form nonlinear optical materials. In this paper, we report on the formation of colloidal Au nanoclusters in fused silica by MeV ion implantation. We present measurements of the Au precipitate size and size distribution as a function of implantation and annealing conditions. Finally, we correlate the microstructural data with measurements of the optical absorption to show the effect of particle size on the intensity of surface plasmon resonance absorption. Preliminary measurements of the nonlinear refractive index are included.

EXPERIMENTAL

Fused silica samples (7940 glass) were implanted by Au at an energy of 2.75 MeV to doses in the range of $3 \times 10^{16}/cm^2$ to $1.5 \times 10^{17}/cm^2$. Substrate temperatures during implantation were in the range from liquid nitrogen temperature (LN_2) to 600°C. Samples were characterized following implantation using 2.3 MeV Rutherford backscattering (RBS), cross-section transmission electron microscopy (TEM), x-ray diffraction, and optical absorption measurements. Differential optical absorption measurements were carried out at RT using a Cary 14 dual beam spectrophotometer with an unimplanted sample in the reference beam. From the absorption measurements, the quantity Kl (K = extinction coefficient, l = path length) was extracted as a function of wavelength using the exponential law of absorption. The optical absorption results are plotted versus photon energy as the extinction coefficient per implanted ion (i.e., as Kl/ion dose) in units of 10^{-17} cm^2/ion.

RESULTS AND DISCUSSION

Figure 1 shows cross section TEM micrographs taken near the edge of the implanted region for a sample implanted to a dose of $1.5 \times 10^{17}/cm^2$ at a substrate temperature of 600°C. In the

low-magnification micrograph (a), one can see that a high density of colloidal precipitates form in the vicinity of the ions end-of-range (~8000 Å). At higher magnification and from the diffraction pattern (b), the individual precipitates are observed to be spherical single crystals of Au, which are randomly oriented relative to each other. In this case, the Au nanocrystals formed during implantation at elevated temperature and the average size is ~130 Å diameter. These are cross-section micrographs, and we cannot measure the nanocrystal volume fraction directly. However, from the optical absorption measurements (to be discussed), we estimate a volume fraction of 7% for the Au nanocrystals in Fig. 1. This is orders-of-magnitude higher than that of Au doped glass.

Figure 2 compares RBS spectra taken from fused silica samples implanted at 600°C and at RT. At RT, the peak in the Au profile occurs at a depth of ~8500 Å, and the full width at half maximum (FWHM) is ~5000 Å. In the sample implanted at 600°C, the profile is slightly narrower (FWHM ~3700 Å), but the peak concentration is greater. This narrowing of the profile presumably occurs due to precipitate growth by Ostwald ripening[10] during the elevated temperature implantation.

Cross-section TEM micrographs showing the Au nanocrystals formed in fused silica during implantation at RT and during subsequent thermal annealing are shown in Fig. 3. Figure 3a shows that a high density of Au nanocrystals form during implantation at RT, but the nanocrystals are very small (less than 20 Å diameter). Annealing in an oxygen atmosphere (c and d) causes the nanocrystals to coarsen and grow, and the size increases as the temperature increases. Surprisingly, the size of Au nanocrystals formed during annealing in an oxidizing atmosphere (d) is much greater than that formed during annealing in a reducing environment (b) for the same time and temperature. This result suggests that the diffusivity of Au is greater during annealing in an oxidizing environment than in a reducing environment. The reason for this is not clear, but it might be related to defect enhanced diffusion. RBS measurements for Au profiles in the as-implanted state and after annealing in either oxygen or hydrogen are virtually identical, showing that very long-range diffusion of Au is not occurring during annealing in either atmosphere.

The size distributions measured for Au nanocrystals in Fig. 1 and Fig. 3 (b, c, and d) are shown in Fig. 4. (Nanocrystals with diameters less than 10–15 Å are not included in the distributions). Following implantation, the nanoclusters are largest for the sample implanted at 600°C. In this case, the distribution is peaked at ~130 Å with a width of ~50 Å on top of a constant background. The sample annealed in oxygen at 1100°C has a nearly flat distribution to ~130 Å, whereas the sample annealed in the reducing atmosphere for the same temperature and time has nanoclusters that are all less than 50 Å in diameter. The sample annealed at 900°C in O_2 has an intermediate size distribution which is in good qualitative agreement with that reported in Ref. 6 for annealing under the same conditions.

It has long been known[11-13] that metallic nanoclusters embedded in dielectrics or aqueous solutions give rise to optical absorption at the surface plasmon resonance frequency, and Fig. 5 shows the effect of nanocluster size on the surface plasmon absorption. Absorption results for the sample implanted at 600°C (shown in Fig. 1) are compared with results from samples implanted at RT in the as-implanted state and after annealing at 1100°C in oxidizing or reducing environments (shown in Fig. 3-a, b, d). (Size distributions are given in Fig. 4 for each of these except the as-implanted sample at RT). Implantation at RT results in very small nanoclusters (Fig. 3a). In this case, the optical absorption varies monotonically with energy, and there is no pronounced absorption band. Samples with larger nanoclusters have an absorption band at a photon energy of ~2.35 eV, and the extinction coefficient per ion increases in magnitude as the particle size increases.

The absorption band at 2.35 eV is the surface plasmon resonance energy predicted by the Mie theory for small gold nanocrystals in silica.[3,11] When the nanocrystal is much smaller than the wavelength of light, then optical extinction is dominated by absorption. To lowest order, the absorption (extinction) coefficient can be expressed in the electric dipole approximation as

$$K\ (cm^{-1}) = \frac{18\pi Q n_d^3}{\lambda} \frac{\varepsilon_2}{(\varepsilon_1+2n_d^2)^2+\varepsilon_2^2} \quad (1)$$

where Q is the volume fraction occupied by the nanocrystals, n_d is the refractive index of the host medium, ε_1 and ε_2 are the real and imaginary parts of the dielectric constant of the bulk metal and λ is the optical wavelength. Equation (1) is a Lorentzian function with a maximum value at the surface plasmon resonance frequency (ω_p) where

$$\varepsilon_1(\omega_p) + 2n_d^2 = 0 \quad (2)$$

Using tabulated optical constants for Au, and n_d (fused silica) = 1.49, then equation (2) predicts a photon energy of 2.34 eV for Au in SiO_2. This is in good agreement with the measured value of 2.35 eV in Fig. 5. A small shift of the surface plasmon resonance to lower energy is expected as the particle size increases, and the data in Fig. 5 is consistent with this.

Figure 5 demonstrates that surface plasmon resonance absorption is dependent on nanocrystal size, and Fig. 2 shows the variation of size with thermal annealing for samples implanted at RT. Nanocrystal size can also be varied by changing the substrate temperature during implantation or by changing the implantation dose during implantation at elevated temperature. Examples of the morphology of Au nanocrystals formed by elevated temperature implantation (400°C) to different doses is shown in Fig. 6. At the two lower doses, there is a very little difference in the size of the Au nanocrystals, but at the high dose, it is clear that the size is somewhat larger. The size distribution gives an average size of ~40 Å diameter for the two lower doses with very few particles in excess of 50 Å diameter. At the higher dose, the average size is ~60 Å diameter, with a few nanocrystals being almost 100 Å diameter. Optical absorption measurements for these samples show a small increase in the extinction coefficient per ion for the high dose sample relative to the two lower doses. The volume fraction occupied by the Au nanocrystals (extracted from the optical absorption data) increases very nearly in proportion to the dose for the samples in Fig. 6. At higher implantation temperatures, there is a significantly larger change of nanocrystal size with dose.

Preliminary measurements of the nonlinear refractive index have been made for the samples shown in Fig. 6. These measurements were carried out using the Z-scan method.[14] This method measures the normalized transmission as a function of laser intensity as the sample is moved through the focal plane of a long focal length lens (150 nm in these experiments). The laser used was a cavity dumped tunable dye laser with a 6 ps pulse duration time. The laser operated at 3.8 MHz, and the average power was 200 mW in the TEM mode. The peak irradiance for a focal spot of 25 μm in radius was 4.5×10^8 W/cm^2. The index of refraction is given by

$$n = n_0 + n_2 I \quad (3)$$

where n_2 is the intensity dependent term. The normalized far field transmission for a small aperture as a function of sample position relative to the focal plane of the lens is shown in Fig. 7 for the sample implanted to 1.5×10^{17}/cm^2 at 400 °C. This signal first decreases then increases in intensity while moving through the focal plane, thus indicating a positive n_2. Table I tabulates values for n_2 extracted from the Z-scan data (using the criteria for critical power at self focusing[15]) for the three samples of Fig. 6 which were implanted at 400°C. All measurements were made at 570 nm, just off the surface plasmon resonance (~530 nm). For small apertures, the Z-scan method measures contributions from both thermal and electronic components and the measurements to date do not distinguish between the components. In Table I, the magnitude of n_2 scales roughly with dose and n_2 is of the order of 10^{-10} cm^2/Watt. This suggests that n_2 scales

linearly with the volume fraction of Au nanocrystals. Such a dependence of the nonlinear susceptibility and n_2 on volume fraction is expected at or near the surface plasmon resonance.[16] Measurements as a function of wavelength and for different particle sizes are in progress and will be reported in the future.

Table I. Nonlinear Refractive Index (at 570 nm) for Au Implanted SiO_2

Dose (ions/cm^2)	3×10^{16}	6×10^{16}	1.5×10^{17}
n_2 (cm^2/Watt)	1.2×10-10	2.4×10-10	4.1×10^{-10}

CONCLUSIONS

MeV implantation of Au into fused silica can be used to create a very high density of Au nanocrystals in fused silica in a shallow layer. The size of the Au nanocrystals varies from less than 20 Å diameter to ~200 Å diameter. The size and size distribution are functions of the implantation and annealing conditions. Implantation at elevated temperature or annealing in an oxidizing environment leads to larger nanocrystals. Annealing in a reducing environment or implantation at lower temperature leads to smaller nanocrystals. The presence of these Au nanocrystals in fused silica leads to surface plasmon resonance absorption whose magnitude is correlated to particle size. Preliminary measurements at 570 nm give a value for n_2 of the order of 10^{-10} cm^2/Watt for particles of ~50 Å diameter and a volume fraction of a few percent.

Research at Oak Ridge National Laboratory is sponsored in part by the Division of Materials Sciences, U.S. Department of Energy, under contract DE-AC05-84OR21400 with Martin Marietta Energy Systems, Inc., and in part by an appointment to the Oak Ridge National Laboratory Postdoctoral Research Program administered by the Oak Ridge Institute for Science and Education. Research at Vanderbilt is administered by the Army Research Office grant DAAH04-93-G-0123.

REFERENCES

1. D. Ricard, P. Roussignol, and C. Flytzanis, Opt. Lett. **10**, 511 (1985).

2. F. Hache, D. ricard, C. Flytzanis, and U. Kreibig, Appl. Phys. **A47**, 347 (1988).

3. G. W. Arnold, J. Appl. Phys. **46**, 4466 (1975).

4. R. H. Magruder, L. Yang, R. F. Haglund, C. W. White, L. Yang, R. Dorsinville, and R. R. Alfando, Appl. Phys. Lett. **62**, 1730 (1993).

5. K. Fukumi, A. Chayahara, M. Satou, J. Hayakawa, M. Hangyo, and S. Nakashima, Jap. J. Appl. Phys. **30**, L742 (1991).

6. K. Fukumi et al., Mat. Res. Soc. Sym. Proc. **235**, 389 (1992).

7. G. Abouchacra, G. Chassagne, and J. Serughetti, Rad. Effects **64**, 189 (1982).

8. C. W. White, D. K. Thomas, R. A. Zuhr, J. C. McCallum, A. Pogany, R. F. Haglund, R. H. Magruder, and L. Yang, Mat. Res. Soc. Sym. Proc. **268**, 331 (1992).

9. R. F. Haglund et al., Proceedings of the 7th International Conference on Radiation Effects in Insulators, Elsevier, Amsterdam (in press).

10. See for example, S. Mantl, Mat. Sci. Reports **8**, 1 (1992).

11. G. Mie, Ann. Physik **25**, 377 (1908).

12. W. T. Doyle, Phys. Rev. **111**, 1067 (1958).

13. R. H. Doremus, J. Chem. Phys. **40**, 2389 (1964); J. Appl. Phys. **37**, 2775 (1966).

14. M. Sheik-Bahae, A. Said, T. Wei, D. J. Hagan, and E. W. VanStryland, IEEE J. Quantum Elect. **26**, 760 (1990).

15. R. W. Boyd, Nonlinear Optics (Academic Press, Boston, Mass.) 1992.

16. F. Hache, D. Ricard, and C. Flytzanis, J. Opt. Soc. Am. **B3**, 1647 (1989).

FIGURE CAPTIONS

Fig. 1. Cross-section TEM micrographs of fused silica implanted by Au (2.75 MeV, $1.5 \times 10^{17}/cm^2$) at 600°C. The high-resolution micrograph (b) was taken from the region where the nanocrystal density is the highest.

Fig. 2. RBS (2.3 MeV He) results showing Au profiles for fused silica samples implanted at RT and at 600°C.

Fig. 3. Cross-section TEM micrographs showing Au nanoclusters formed during Au (2.75 MeV, $1.5 \times 10^{17}/cm^2$) implantation of fused silica at RT (a) and during subsequent thermal processing (b, c, d) of the as-implanted samples.

Fig. 4. Size distribution for Au nanocrystals in fused silica following Au (2.75 MeV, $1.5 \times 10^{17}/cm^2$) implantation. The top distribution was measured following implantation at 600°C. The other three distributions were measured after annealing samples implanted at RT.

Fig. 5. Optical absorption for fused silica samples implanted by Au (2.75 Mev, $1.5 \times 10^{17}/cm^2$). The annealed samples were implanted at RT.

Fig. 6. Cross-section TEM micrographs for Au (2.75 MeV, $1.5 \times 10^{17}/cm^2$) implanted into fused silica at 400°C. Implantation doses are indicated.

Fig. 7. Z-scan measurements for Au (2.75 MeV, $1.5 \times 10^{17}/cm^2$, 400°C) implanted fused silica.

Au (2.75 MeV, $1.5 \times 10^{17}/cm^2$, 600°C) in Fused Silica

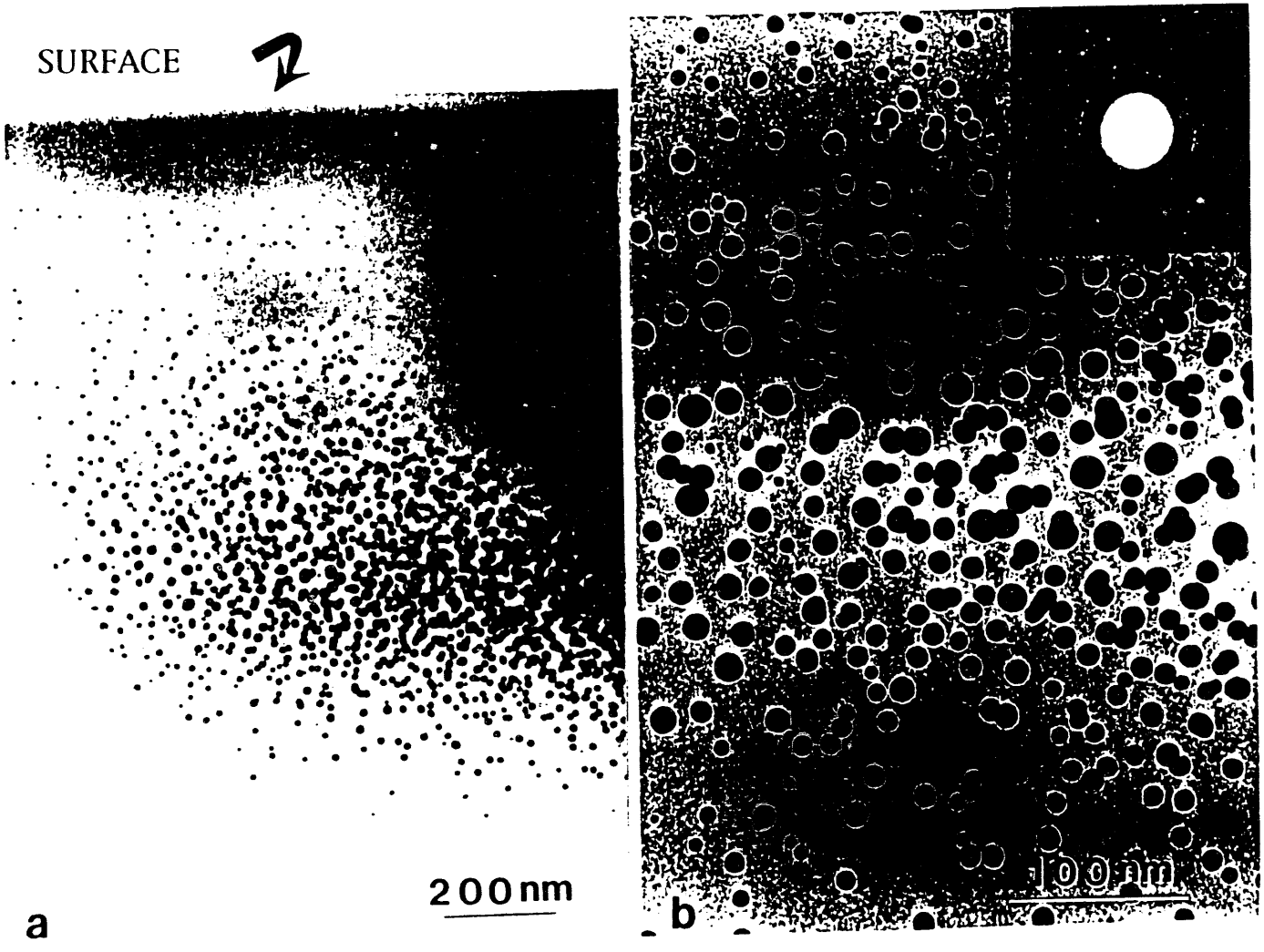

Figure 1.

ORNL-DWG 93M-5408

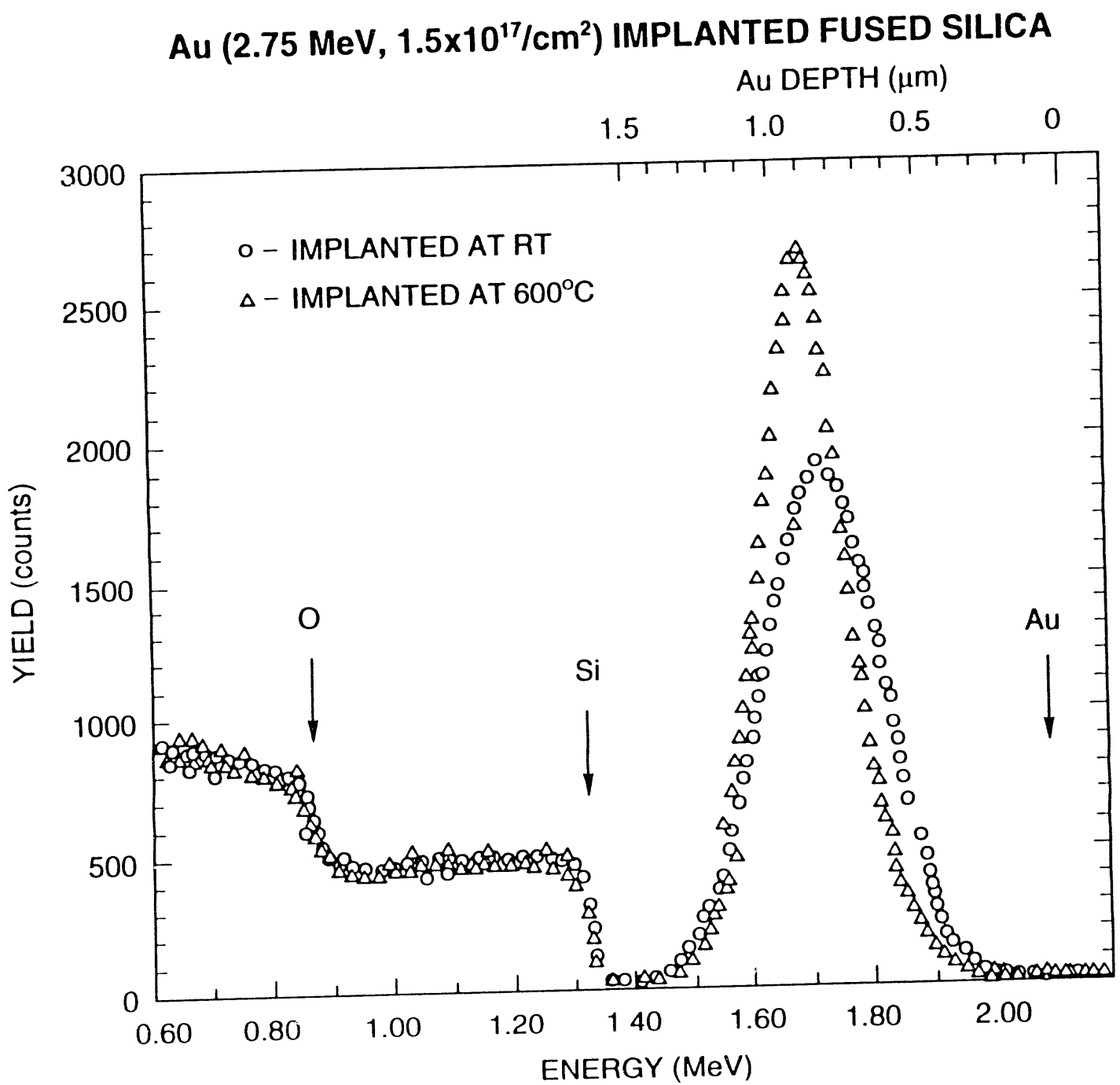

Au (2.75 MeV, $1.5 \times 10^{17}/cm^2$) in Fused Silica

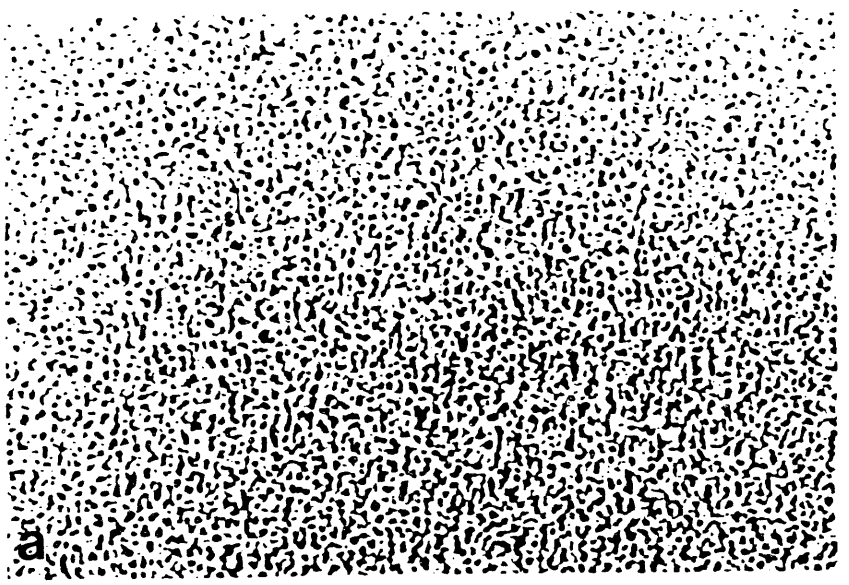

As Implanted

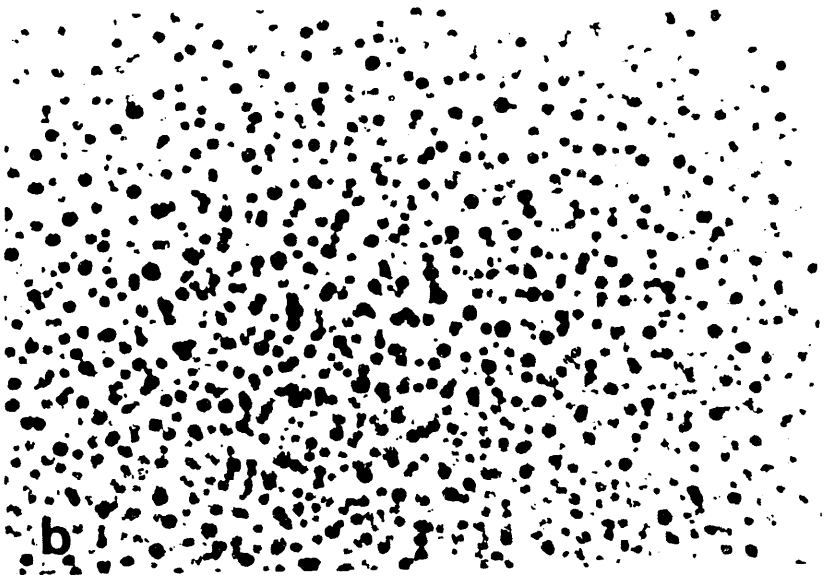

Annealed 1100°C/2.2h/$Ar+H_2$

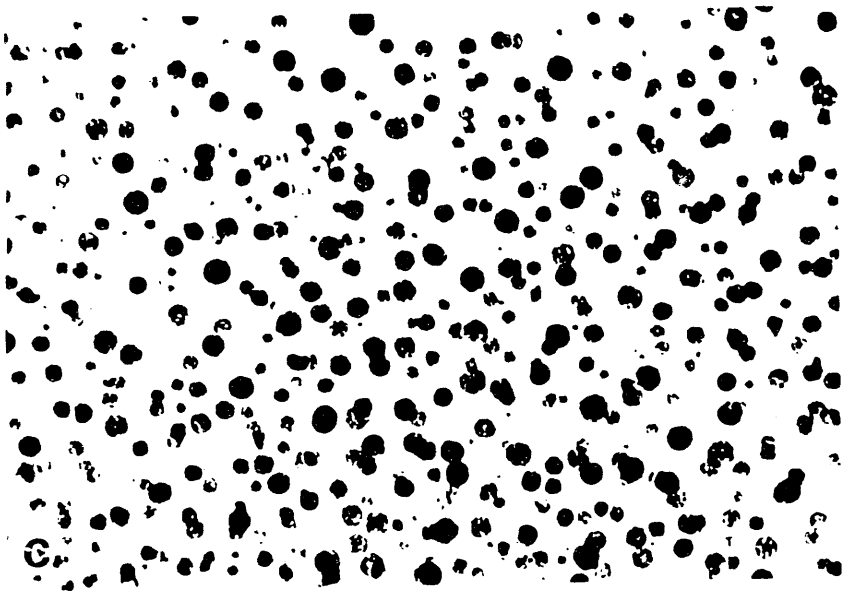

Annealed 900°C/5h/O_2

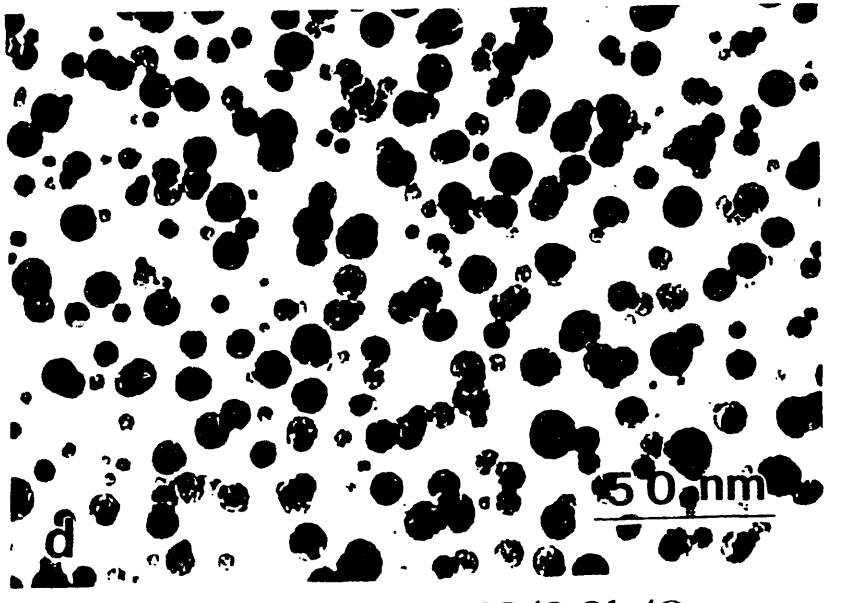

Annealed 1100°C/2.2h/O_2

ORNL-DWG 93M-6047

Au (2.75 Mev, 1.5 x $10^{17}/cm^2$) IMPLANTED FUSED SILICA

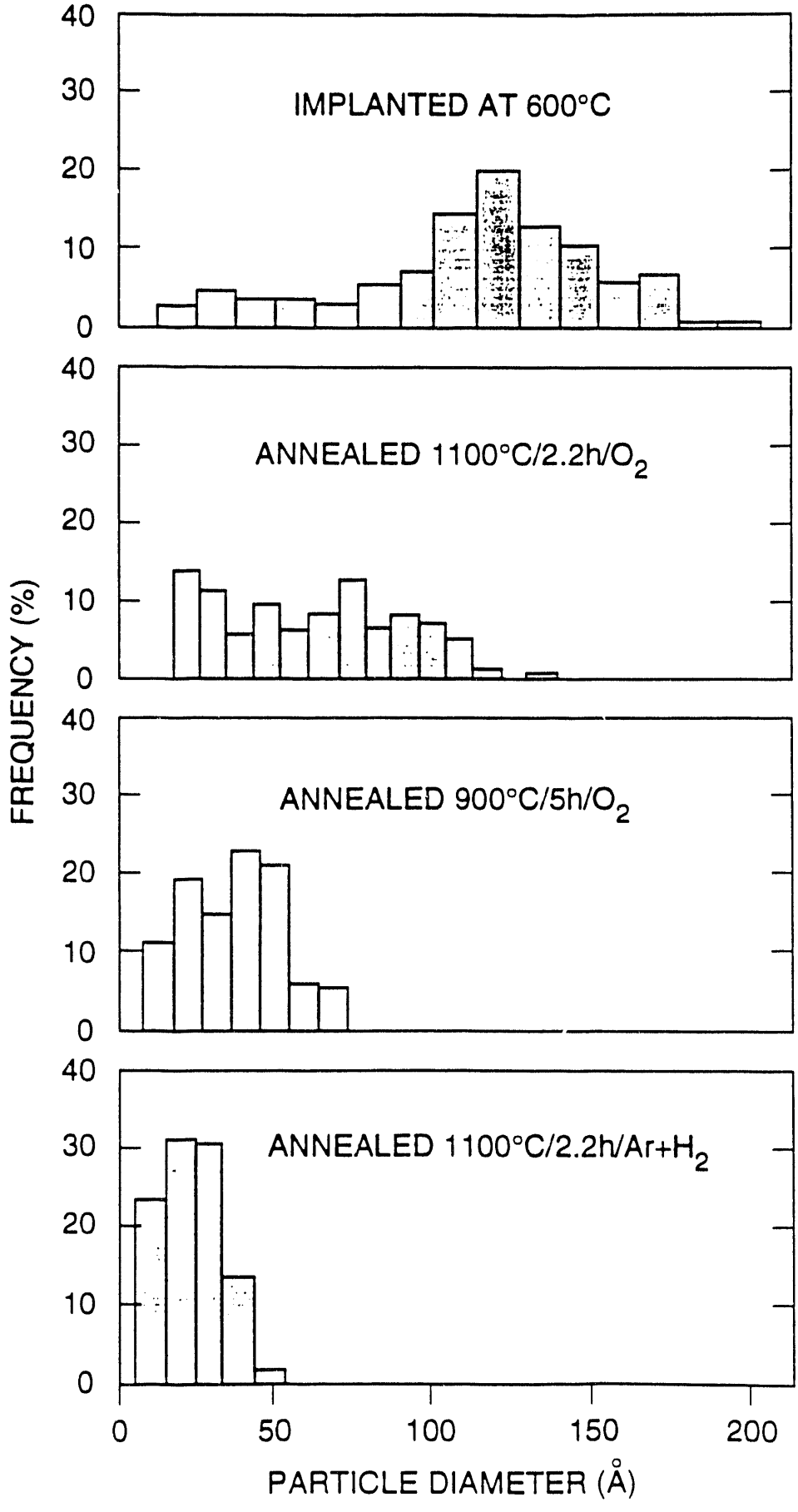

ORNL-DWG 93M-5353R

Au NANOCLUSTERS FORMED BY MeV ION IMPLANTATION

Au (2.75 MeV, 1.5 x 10^{17} / cm^2) IMPLANTED FUSED SILICA

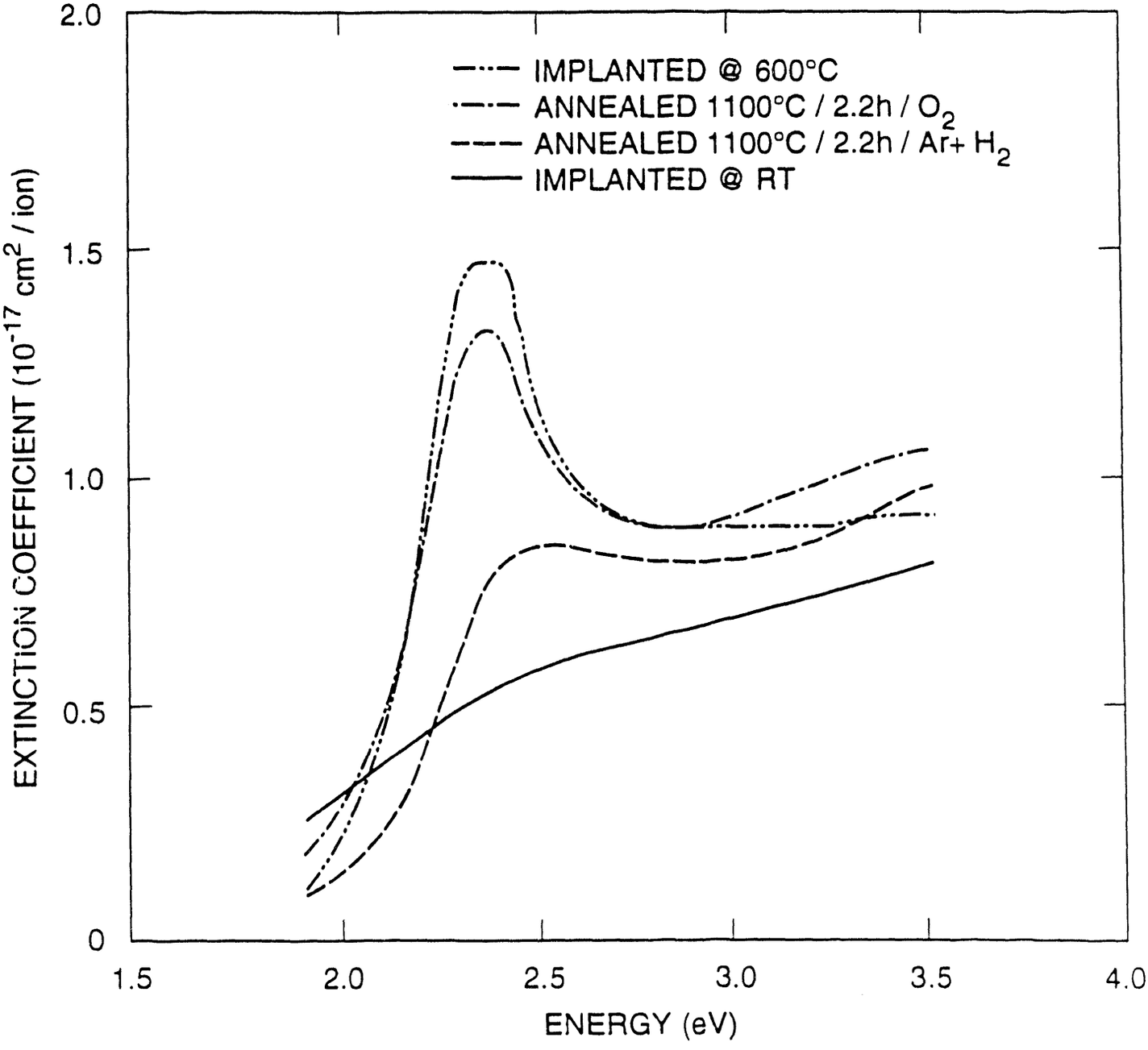

- **Intensity of surface plasmon resonance absorption depends on precipitate size.**

Figure 5

Au (2.75 MeV, 400°C) in Fused Silica

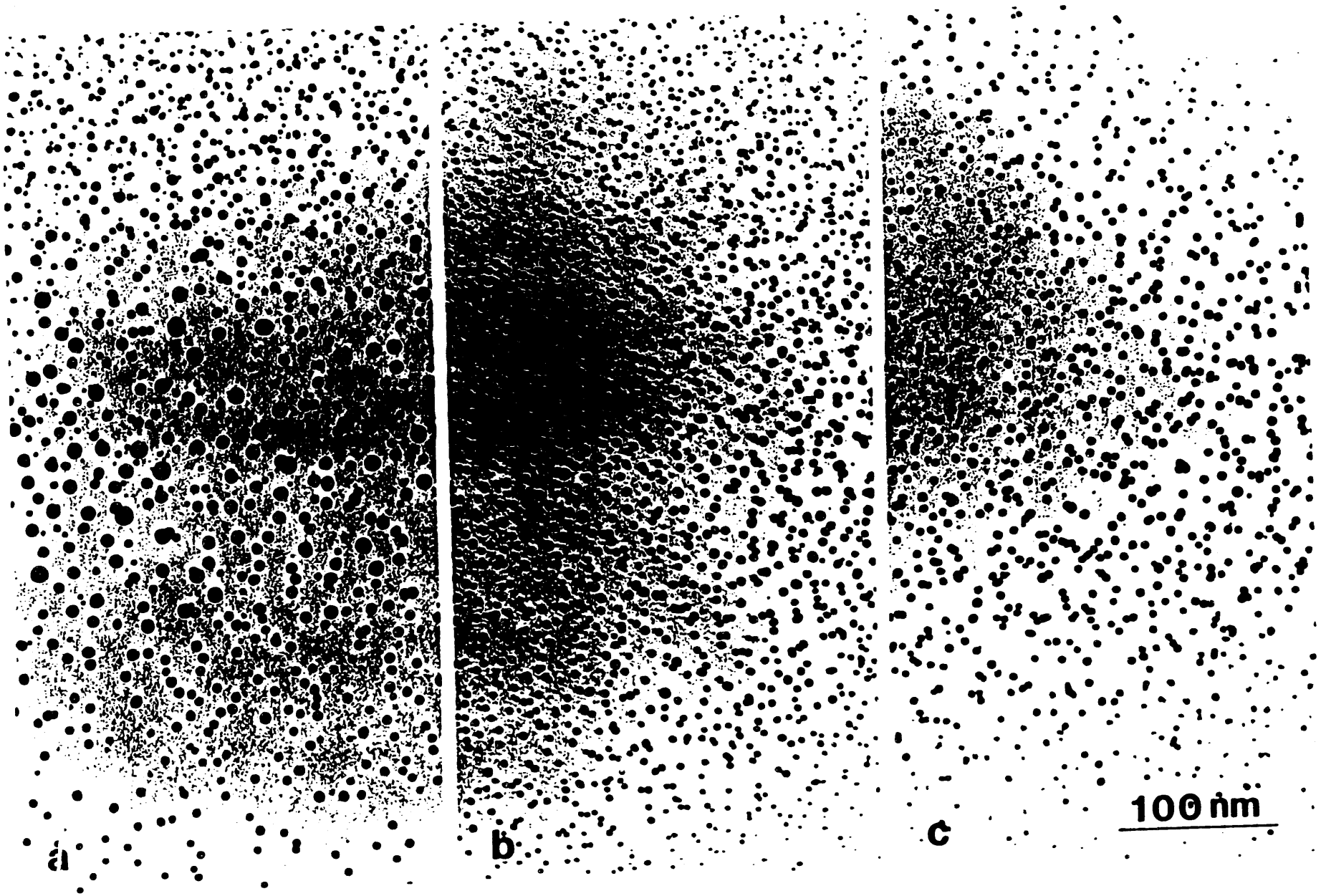

$1.5 \times 10^{17}/cm^2$ $6 \times 10^{16}/cm^2$ $3 \times 10^{16}/cm^2$

ORNL-DWG 93M-15871

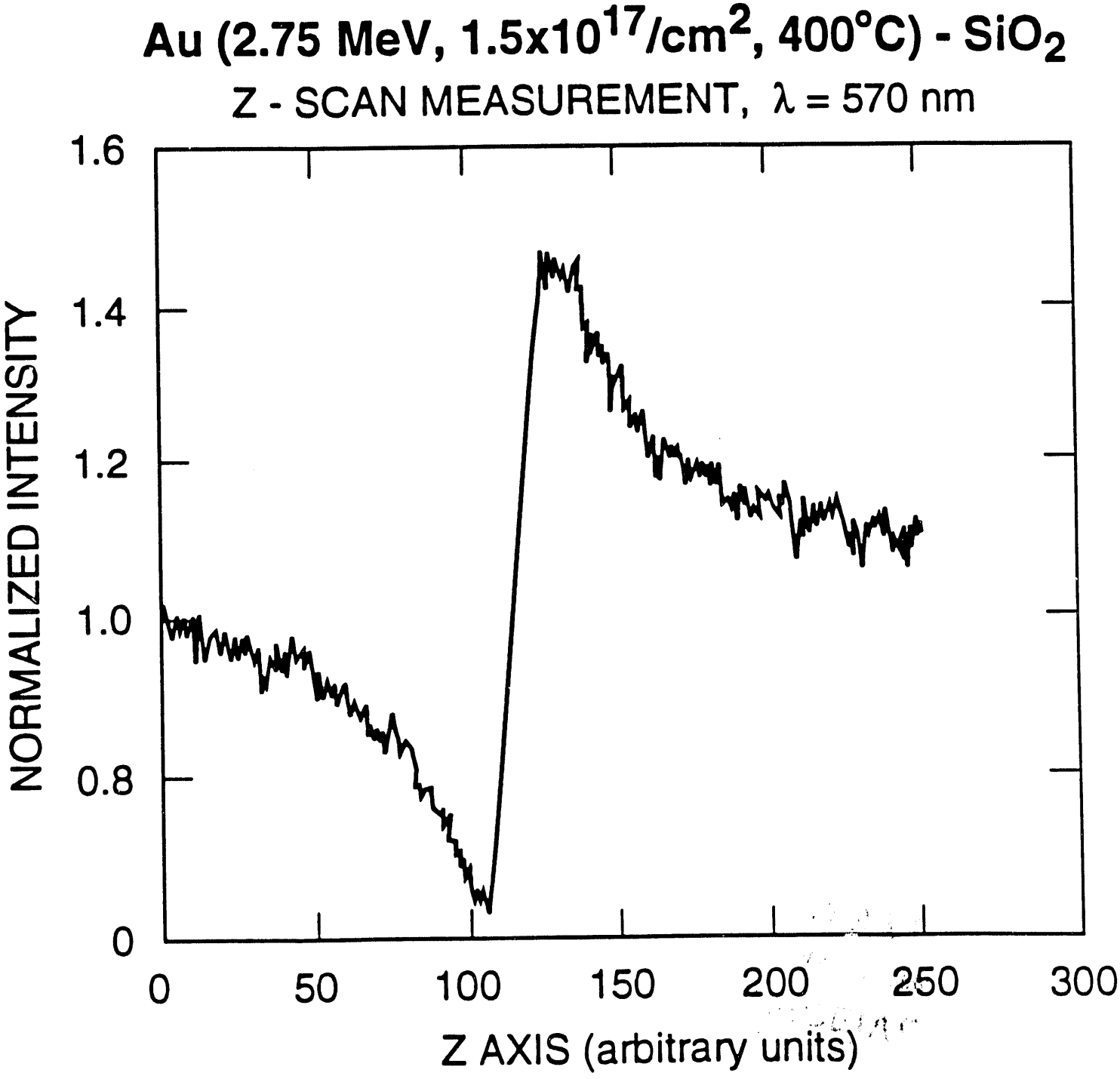

Figure 7

END

DATE
FILMED
2123194